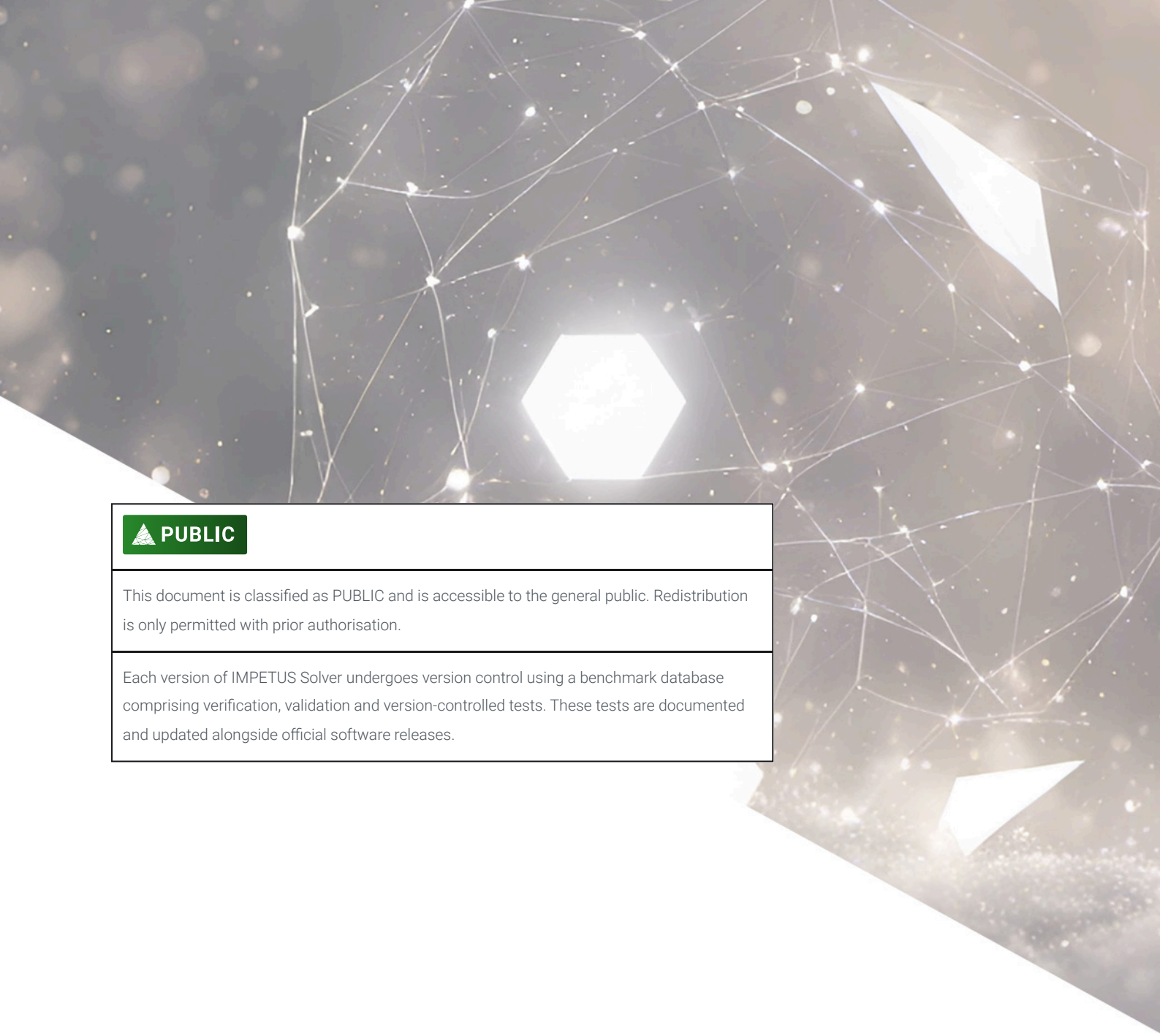

PUBLIC

This document is classified as PUBLIC and is accessible to the general public. Redistribution is only permitted with prior authorisation.

Each version of IMPETUS Solver undergoes version control using a benchmark database comprising verification, validation and version-controlled tests. These tests are documented and updated alongside official software releases.

Validation - Close-Range Blast Loading

Documentation

Version 11.0.0

June 15, 2026

IMPETUS
driving precision

Document revisions:

Revision	Date	Comments
10	2025-02-04	Updated tables
9	2024-12-02	Updated tables
8	2024-10-07	Updated tables
7	2023-10-02	Updated tables
6	2023-02-28	Updated tables and added CFD tests
5	2022-12-01	Updated tables
4	2017-09-04	Updated tables in introduction
3	2017-08-18	Added: Held (2002), Weaver and Walters (1987)
2	2016-08-23	Added: Rigby (2016)
1	2016-03-15	New color scheme and font for all plots
0	2015-11-02	First publication

Validation - Close-Range Blast Loading

Introduction

This document presents validation tests on close-range blast loading modeled with the discrete particle module.

Numerical models of experiments are created and evaluated against the experimental results. Experimental data is gathered from several scientific studies reported in literature and common for the investigated cases is the scaled stand-off distance is less than one. All studies reported here have investigated the full interaction between high explosives, possibly sand and air and metal plate structures.

Version control

The tests presented in this document are subjected to version control, meaning that the models are run and evaluated prior to release of a new solver. This document is updated in conjunction with official releases of the software.

Discrete particle module

For close-range blast loading applications, a discrete particle-based approach is used to treat high explosives, air, and sand. All three particle types can interact in a simulation. The particles interact with structures represented by finite elements. Since the method is particle-based, the contact treatment is very efficient compared to the coupled Eulerian-Lagrangian analyses. The particle-based approach is applicable for close-range blast loading applications, where the scaled stand-off distance is less than two.

The discrete particle module comes with several calibrated explosives, presented in detail and with verification in the document "Verification - Calibrated Explosives". Sand is available as either dry or wet. The dry sand is modeled with a density of $\mathbf{1620}\ \boldsymbol{kg/m^3}$ and is configured with a friction constant, while the wet sand has a density of $\mathbf{2020}\ \boldsymbol{kg/m^3}$ and is configured with both friction and damping. The wet sand is designed for fully saturated sand (moisture content > 20%).

CFD method

Additonally, the airblast tests which do not contain any sand are modelled with the CFD method for comparison. The CFD solver bridges the gap between Discrete Particles (applicable for close range blast and contact detonations) and the semi-empirical pressure-time history curves in *LOAD_AIR_BLAST (suitable for large stand-off distances).

Overview of tests

Comparable conditions in the tests have been normalized using the Hopkinson scaling method: Each parameter has been divided by the cube root of the charge mass $(\sqrt[3]{kg})$. For the experiments that used explosives other than TNT, the TNT equivalent was calculated prior to normalization. The normalized conditions for the air blast tests are showed in Table 1. while the tests with charges buried in sand is presented in Table 2. The density and moisture of the different sand types used in the experiments are displayed in Table 3. Even though the features of the sand are decisive, the two presets are mainly used. The density is however adjusted to match the density of the sand used in the experiments.

Abbreviation	Explaination
W_{TNT}	- TNT equivalent of original charge mass.
SoD	- Stand-off distance, measured from face of charge to face of impacted plate.
HoT	- Height-of-target. Distance between face of target and boundary of sand domain.
DoB	- Depth-of-burial. Distance between boundary of sand domain and face of charge.
A_T	- Area of target plate that is exposed to the blast.
Subscript $_S$	- Normalized distances.

Experiment		Physical distances 	Physical distances 	Scaled distances 	Scaled distances 
Spranghers et al. (2013)	0.041	0.25	0.3 • 0.3	0.73	0.41
Neuberger et al. (2007)	30 70 70	0.40 0.40 0.26	$\pi \cdot 1^2$	0.13 0.10 0.06	13.6 17.7 29.5
Wadley et al. (2011)	0.2	0.12 0.17 0.22	0.4 • 0.4	0.21 0.29 0.38	1.90 1.38 1.05
Neuberger et al. (2009)	15	1.00	$\pi \cdot 0.5^2$	0.41	2.16
Zakrisson et al. (2011)	1	0.25	0.6 • 0.6	0.25	2.40
Held et al. (2002)	2.14 2.14 2.14 1.22	0.10 0.05 0.075 0.10	$\pi \cdot 0.076^2$	0.78 0.39 0.58 0.09	0.17 0.35 0.23 1.50

Experiment		Physical distances 	Physical distances 	Scaled distances 	Scaled distances 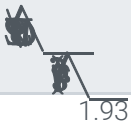
	1.22 1.22 2.65 2.65	0.075 0.05 0.10 0.05		0.07 0.05 0.07 0.04	1.93 2.70 1.93 3.38

Table 1. Normalized experiment distances for the air blast tests.

Experiment	Sand	W_{TNT} (kg)	Physical distances SoD (m)	Physical distances HoT (m)	Physical distances DoB (m)	Physical distances A_T (m^2)	Scaled distances SoD_s $(\frac{m}{\sqrt[3]{kg}})$
Zakrisson et al. (2012)	user user user dry	1	0.246 0.296 0.385 0.296	0.246 0.246 0.235 0.246	0 0.05 0.15 0.05	0.6^2	0.246 0.296 0.385 0.296
Neuberger et al. (2007)	dry	30 30 30 30 50 50 50 50	0.38 0.46 0.56 0.64 0.42 0.47 0.52 0.62	0.38 0.46 0.56 0.64 0.42 0.47 0.52 0.62	0	$\pi \cdot 1^2$	0.12 0.15 0.18 0.21 0.11 0.13 0.14 0.17
Anderson et al. (2011)	dry	0.64	0.25 0.35 0.20 0.25	0.20 0.30 0.15 0.20	0.05	0.8^2	0.29 0.41 0.23 0.29
Rigby et al. (2016)	dry	0.105	0.133 0.168	0.105 0.140	0.028	$\pi \cdot 0.7^2$	0.28 0.36
Wadley et al. (2011)	dry dry dry wet wet wet	0.2	0.12 0.17 0.22 0.12 0.17 0.22	0.07 0.12 0.17 0.07 0.12 0.17	0.05	0.4^2	0.21 0.29 0.38 0.21 0.29 0.38

Table 2. Normalized experiment distances for tests with charges buried in sand.

Experiment	Experiment Density ρ (kg/m^3)	Experiment Moisture (mass - %)	Experiment Boundaries (comment)	Numerical Type (dry/wet/user)	Numerical Density ρ (kg/m^3)
Zakrisson et al. (2012)	1862 ± 40 1771 ± 5	7 ± 1.1 0	box	user dry	1862 1620
Neuberger et al. (2007)	not given	(dry)	buried	dry	1620
Anderson et al. (2011)	1370 ± 30	7	cylinder	dry user	1620 1370
Rigby et al. (2016)	1640	2.5	cylinder	dry	1620
Wadley et al. (2011)	1620 2020	0 24.7	sphere	dry wet	1620 2020

Table 3. Sand properties in the different tests.

A. Neuberger et al. (2007)

Scaling the Response of Circular Plates Subjected to Large and Close-Range Spherical Explosions

In this investigation the results from Neuberger et al (2007) are compared with numerical results from simulations. These tests consider circular plates subjected to large and close-range blast loading from spherical TNT charges. Part I of the original investigation treats explosions in air whereas Part II considers buried charges. A total of 22 different tests are investigated, configured as described in Table 1. Part I and II are used to distinguish between the articles given in the references. Figure 1 shows the two different models used in this investigation: the air blast model and the model for buried charges.

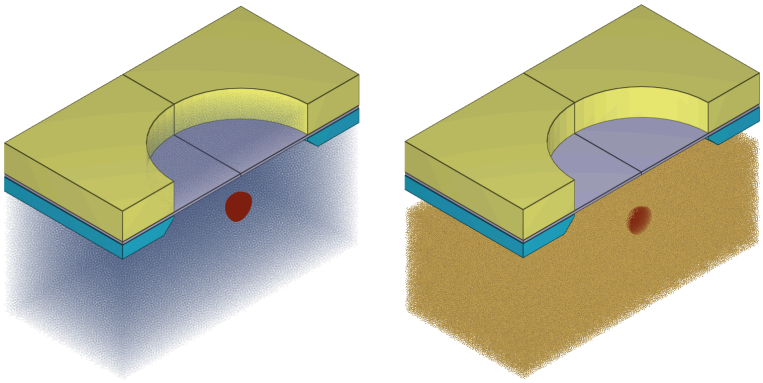

Figure 1. Model to the left is used in the air blast tests (Test 1-6) and model to the right is used in the tests with a buried charge (Test 7-22).

Test	Part	Sand	S	t	D	W	R	t/S	D/S	W/S	R/S
1	I	0	2	0.04	2	30	0.4	0.02	1	3.75	0.2
2	I	0	4	0.04	2	30	0.4	0.01	0.5	0.469	0.1
3	I	0	2	0.04	2	70	0.4	0.02	1	8.75	0.2
4	I	0	4	0.04	2	70	0.4	0.01	0.5	1.094	0.1
5	I	0	2	0.04	2	70	0.26	0.02	1	8.75	0.13
6	I	0	4	0.04	2	70	0.26	0.01	0.5	1.094	0.065
7	II	dry	2	0.04	2	30	0.42	0.02	1	3.75	0.21
8	II	dry	4	0.04	2	30	0.42	0.01	0.5	0.469	0.105
9	II	dry	2	0.04	2	30	0.5	0.02	1	3.75	0.25
10	II	dry	4	0.04	2	30	0.5	0.01	0.5	0.469	0.125
11	II	dry	2	0.04	2	30	0.6	0.02	1	3.75	0.3
12	II	dry	4	0.04	2	30	0.6	0.01	0.5	0.469	0.15
13	II	dry	2	0.04	2	30	0.7	0.02	1	3.75	0.35
14	II	dry	4	0.04	2	30	0.7	0.01	0.5	0.469	0.175
15	II	dry	2	0.04	2	50	0.5	0.02	1	6.25	0.25
16	II	dry	4	0.04	2	50	0.5	0.01	0.5	0.781	0.125
17	II	dry	2	0.04	2	50	0.55	0.02	1	6.25	0.275
18	II	dry	4	0.04	2	50	0.55	0.01	0.5	0.781	0.138
19	II	dry	2	0.04	2	50	0.6	0.02	1	6.25	0.3
20	II	dry	4	0.04	2	50	0.6	0.01	0.5	0.781	0.15

Test	Part	Sand	S	t	D	W	R	t/S	D/S	W/S^3	R/S
				mm	mm	kg	mm	mm	mm	kg	mm
21	II	dry	2	0.04	2	50	0.7	0.02	1	6.25	0.35
22	II	dry	4	0.04	2	50	0.7	0.01	0.5	0.781	0.175

Table 1. Configuration of each test (S = scale, t= plate thickness, D = aperture, W = charge mass, R= stand-off distance measured from center of charge to plate face.

The target plate is modeled with material data from the referenced article and the frame is modeled as rigid. All cases are modeled with quarter symmetry and a total of 500k discrete particles. Air is included in the air blast tests while omitted in the test with a buried charge. There is no information regarding the density of the dry sand used in the experiments so the preset "dry" was selected with the default density.

The maximum central deflection of the plates was measured during the experiments. A comparison between the numerical and experimental results is given in Table 2.

Run	Part	Sand	Max deflection Experiment	Max deflection Simulation	Error (%)
			mm	mm	
1	I	0	0.054	0.039	-27.8
2	I	0	0.026	0.019	-26.9
3	I	0	0.107	0.074	-30.8
4	I	0	0.048	0.038	-20.8
5	I	0	0.165	0.117	-29.1
6	I	0	0.074	0.058	-21.6
7	II	dry	0.116	0.109	-6.0
8	II	dry	0.052	0.054	3.8
9	II	dry	0.094	0.094	0.0
10	II	dry	0.045	0.047	4.4
11	II	dry	0.080	0.083	3.8

Run	Part	Sand	Max deflection Experiment	Max deflection Simulation	Error (%)
12	II	dry	0.039	0.040	2.6
13	II	dry	0.070	0.072	2.9
14	II	dry	0.035	0.036	2.9
15	II	dry	0.160	0.129	-19.4
16	II	dry	0.070	0.063	-10.0
17	II	dry	0.130	0.119	-8.5
18	II	dry	0.060	0.060	0.0
19	II	dry	0.110	0.112	1.8
20	II	dry	0.052	0.056	7.7
21	II	dry	0.092	0.100	8.7
22	II	dry	0.044	0.049	11.4

Table 2. Maximum center deflection (Discrete Particle Method).

A convergence study regarding the number of discrete particles used was done for Test 1 and Test 7 with results showed in Figure 2 and 3. For version control, 500k particles are used.

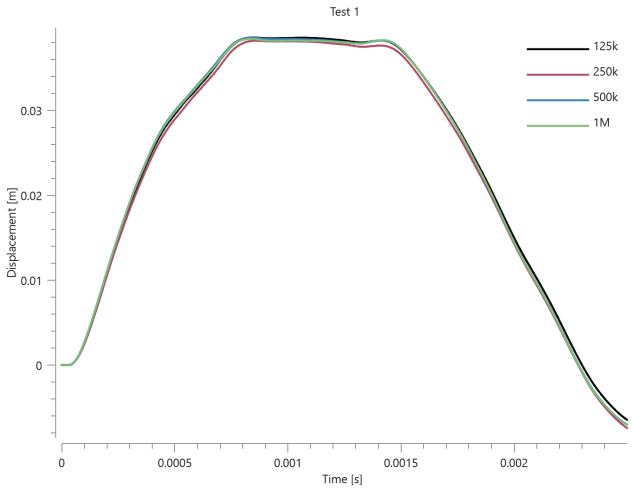

Figure 2. Displacement vs. time for simulations of Test 1 with 125k, 250k, 500k and 1M particles.

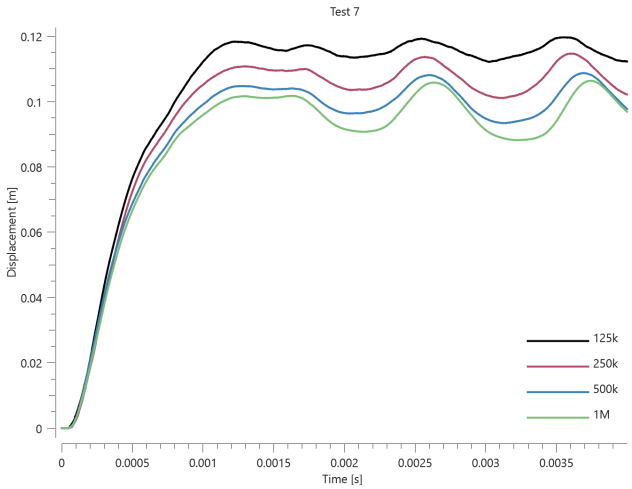

Figure 3. Displacement vs. time for simulations of Test 7 with 125k, 250k, 500k and 1M particles.

The maximum central deflection of the plates from the CFD method was conducted for test 1-6. A comparison between the numerical and experimental results is given in Table 3.

Run	Part	Sand $0/dry$	Max deflection Experiment (m)	Max deflection Simulation (m)	Error (%)
1	I	0	0.054	0.040	-25.9
2	I	0	0.026	0.020	-23.1
3	I	0	0.107	0.077	-18.0
4	I	0	0.048	0.040	-16.7
5	I	0	0.165	0.118	-28.5
6	I	0	0.074	0.059K	-20.3

Table 3. Maximum center deflection (CFD Method).

A convergence study regarding the number of CFD cells was done for Test 1 with results showed in Figure 4. For version control, 0.5 cm sized cells are used.

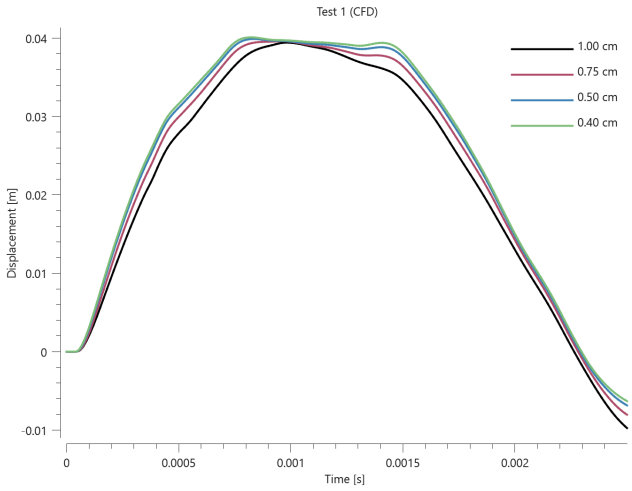

Figure 4. Displacement vs. time for simulations of Test 1 with 1 cm, 0.75 cm, 0.50 cm and 0.40 cm sized CFD cells.

References

[1] - A. Neuberger, S. Peles, D. Rittel, Scaling the Response of Circular Plates Subjected to Large and Close-range Spherical Explosions. Part I: Air-blast loading, International Journal of Impact Engineering, Volume 34, Issue 5, May 2007, Pages 859-873.

[2] - A. Neuberger, S. Peles, D. Rittel, Scaling the Response of Circular Plates Subjected to Large and Close-range Spherical Explosions. Part II: Buried charges, International Journal of Impact Engineering, Volume 34, Issue 5, May 2007, Pages 874-882.

TESTS

This benchmark is associated with 40 tests.

A. Neuberger et al. (2009)

Springback of circular clamped armor steel plates subjected to spherical air-blast loading

In this investigation the results from Neuberger et al (2009) are compared with numerical results from simulations. The setup is a clamped, circular RHA steel plate exposed to blast loading in air from a spherical charge of 15 kg TNT at a stand-off distance of 1 m (centre of charge), see Figure 1.

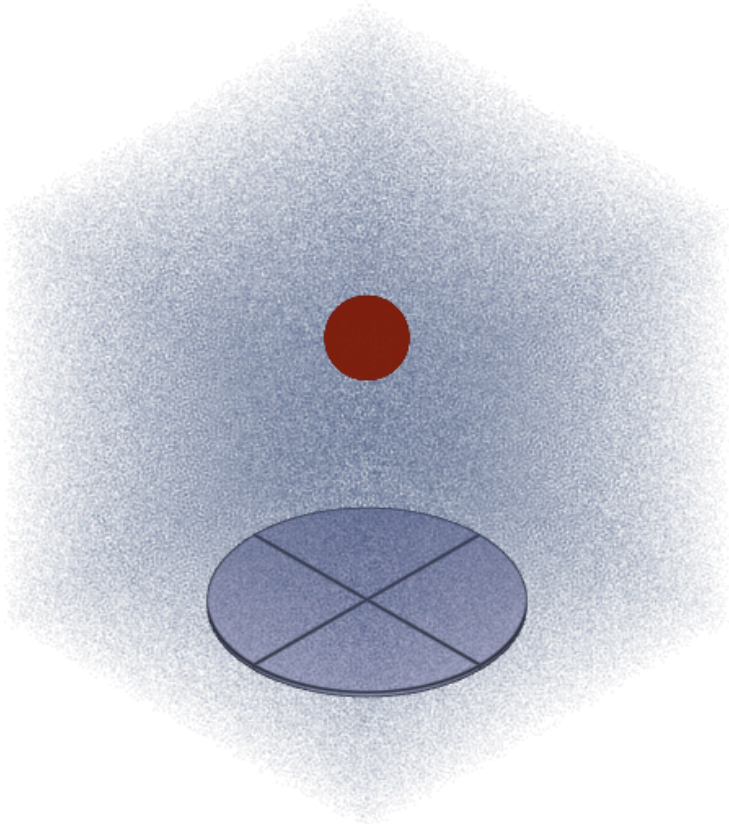

Figure 1. The numerical model of the experiment with the explosive charge, surrounding air and the target plate of RHA.

The air and explosive charge are modeled with total of 1M particles and the steel plate is modeled in accordance to the referenced article. The edges of the target plate are fixed in XYZ which is a simplification of the clamped condition used in the experiment. Quarter symmetry is utilized to reduce computational time.

The maximum central deflection of the plates is measured during the experiments. The deflection found from the simulation is compared to the experimental result in Table 1 and Figure 2.

Test	Exp. deflection (m)	Num. deflection (m)	Error (%)
Air blast	0.034	0.028	-17.6

Table 1. Maximum center deflection (Discrete Particle Method).

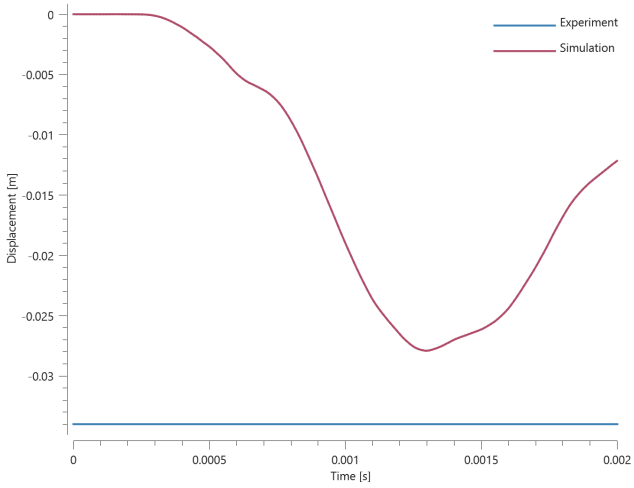

Figure 2. Displacement vs. time from simulation together with max displacement from experiment.

An analysis of the sensitivity to the number of discrete particles used is presented in Figure 3. For version control, 1M particles are used.

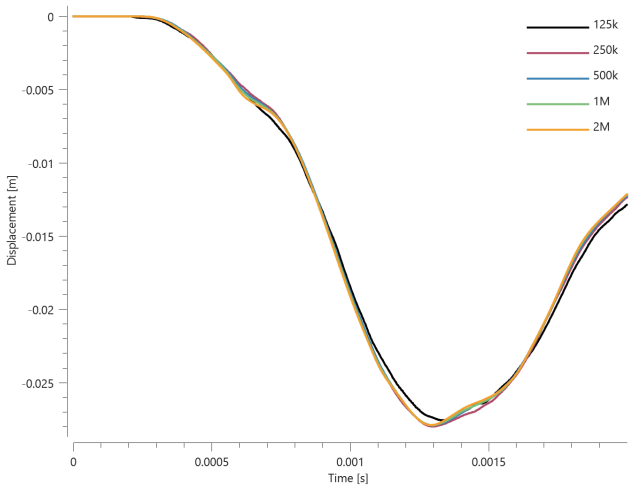

Figure 3. Displacement vs. time from simulations with 125k, 250k, 500k, 1M and 2M particles.

The maximum central deflection of the plates from the CFD method compared to the experimental results is given in Table 2 and Figure 4.

Test	Exp. deflection (m)	Num. deflection (m)	Error (%)
Air blast	0.034	0.027	-20.6

Table 2. Maximum center deflection (CFD Method).

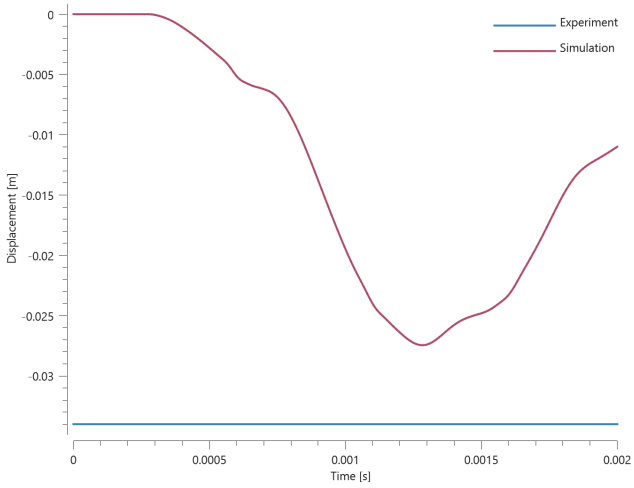

Figure 4. Displacement vs. time from simulation together with max displacement from experiment.

A convergence study regarding the number of CFD cells used is presented in Figure 5. For version control, 0.5 cm sized cells are used.

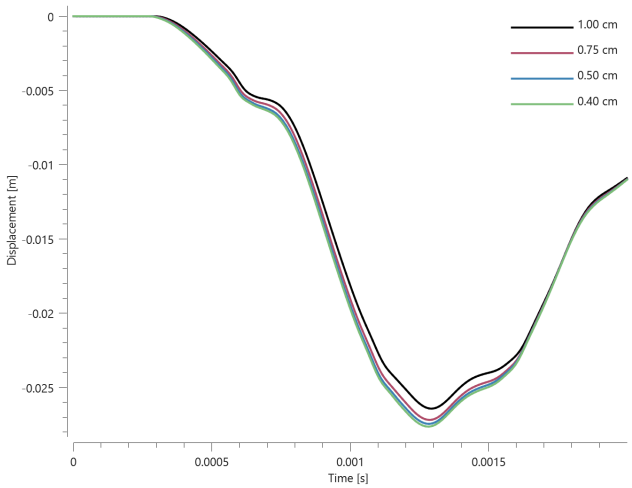

Figure 5. Displacement vs. time from simulations with 1.00 cm, 0.75 cm, 0.50 cm and 0.40 cm sized CFD cells.

References

[1] - A. Neuberger, S. Peles, D. Rittel, Springback of circular clamped armor steel plates subjected to spherical air-blast loading, International Journal of Impact Engineering, Volume 36, Issue 1, January 2009, Pages 53-60.

[2] - L. Olovsson, A.G. Hanssen, T. Børvik, M. Langseth, A particle-based approach to close-range blast loading, European Journal of Mechanics - A/Solids, Volume 29, Issue 1, January - February 2010, Pages 1-6.

TESTS

This benchmark is associated with 11 tests.

B. Zakrisson et al. (2011)

Numerical Simulations of Blast Loads and Structural Deformation from Near-Field Explosions

In this investigation the results from Zakrisson et al (2011) are compared with numerical results from simulations. The setup is a charge set off close to a steel plate. The peak displacement of the plate is measured. Two different blast loading cases are investigated: (1) a charge is located above the plate, and the plate rests freely on a stiff, cylindrical steel rig, and (2) a charge located within a steel pot beneath the plate, which is now fastened to the rig. The numerical models of both setups are displayed in Figure 1.

The aim of the second experiment is to replicate the conditions of the NATO Standard, where an explosive located in a steel pot is suggested as an alternative test method instead of positioning in sand. Please refer to the Zakrisson (2011) III benchmark for the experiments with sand included. Stand-off distances (SoD) are 250 mm and 255 mm, respectively, measured from the closest face of the charge to the plate. The charge is a 750g cylinder of m/46, with a diameter-to-height ratio of 3.

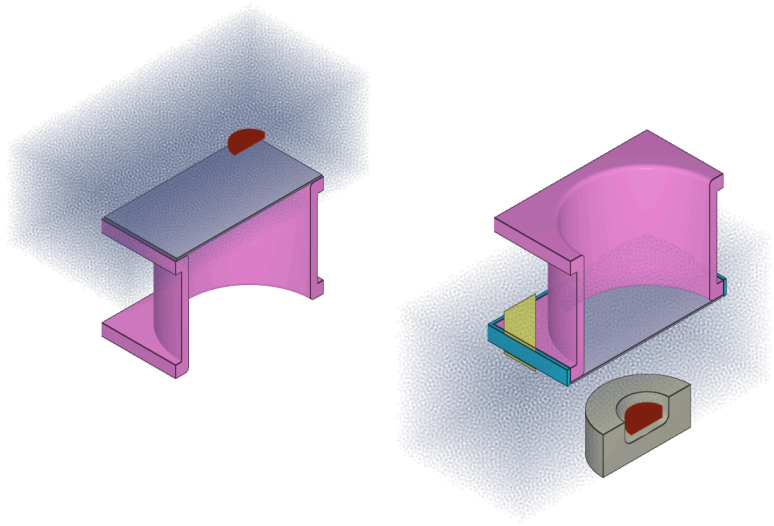

Figure 1. To the left: model of test with airblast. To the right: model of test with charge in steel pot.

The conditions in the experiments are presented in Table 1. In the experiments, different contact conditions between plate and rig was investigated, namely: dry and lubricated. The result from the dry tests is used for comparison with simulations.

Test	Steel pot depth (mm)	Steel pot radius (mm)	SoD (m)
1-5	-	-	0.250
11-12	66	87	0.255

Table 1. Experiment conditions.

The target plate of steel is modeled in accordance to the referenced literature while the rig and the steel pot is modeled as rigid. The air and explosive charge are modeled with a total of 500k particles which is determined from the sensitivity study in which quarter symmetry is being used.

The maximum deflection of the center part of the plate is measured during the experiments. A comparison between the numerical and experimental results is presented in Table 2 and Figure 2 and Figure 3.

Test	Maximum deflection Experiment (m)	Maximum deflection Simulation (m)	Error (%)
1-5	0.066	0.048	-27.3
11-12	0.124	0.128	3.2

Table 2. Maximum deflection (Discrete Particle Method).

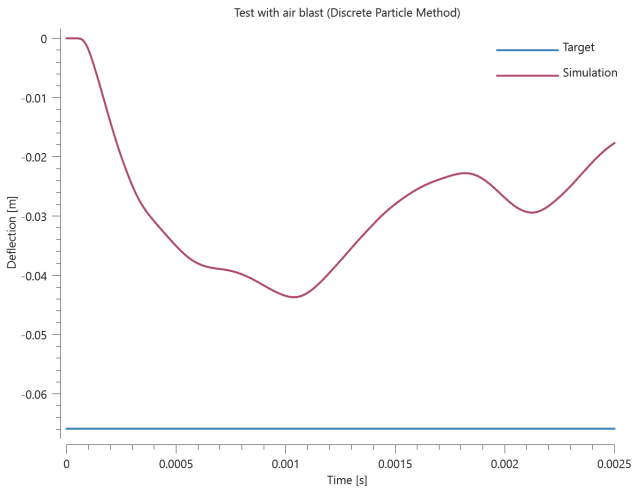

Figure 2. Deflection vs. time from simulation together with max deflection from experiment.

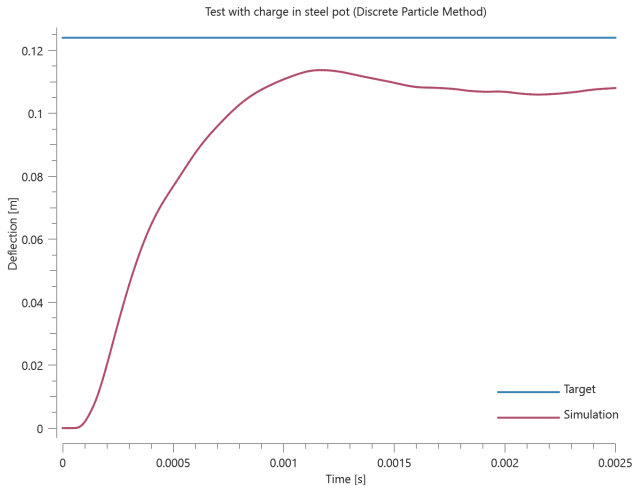

Figure 3. Deflection vs. time from simulation together with max deflection from experiment.

The models sensitivity to the number of particles used is investigated with results presented in Figure 4 and 5. Quarter symmetry is used.

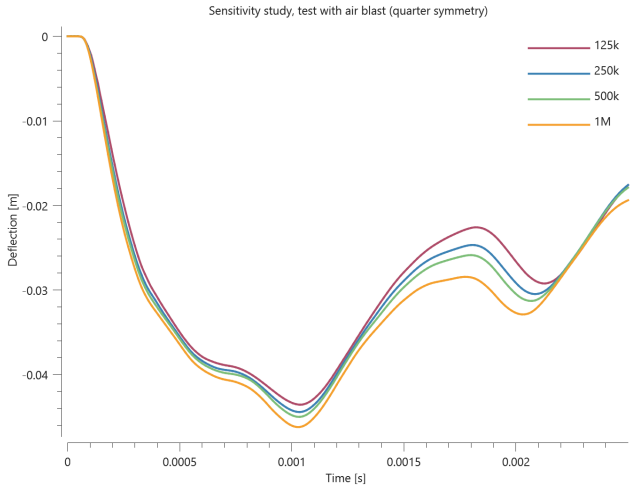

Figure 4. Deflection vs. time from simulations with 125k, 250k, 500k and 1M particles.

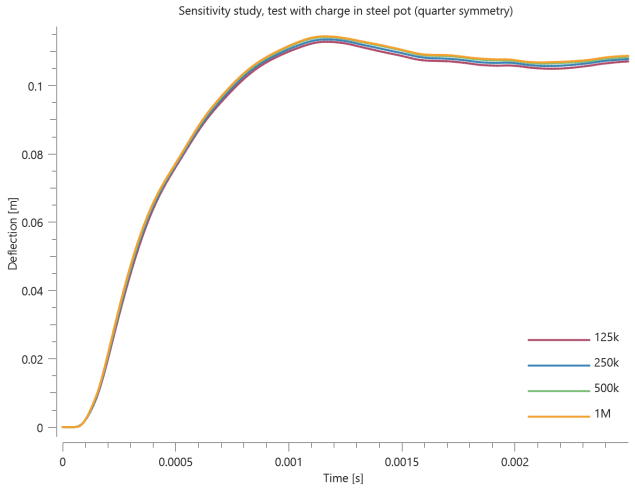

Figure 5. Deflection vs. time from simulations with 125k, 250k, 500k and 1M particles.

The maximum deflection of the center part of the plate from the CFD method compared to the experimental results is presented in Table 3 and Figure 6 and 7.

Test	Maximum deflection Experiment (m)	Maximum deflection Simulation (m)	Error (%)
1-5	0.066	0.058	-12.1
11-12	0.124	0.152	22.6

Table 3. Maximum deflection (CFD Method)

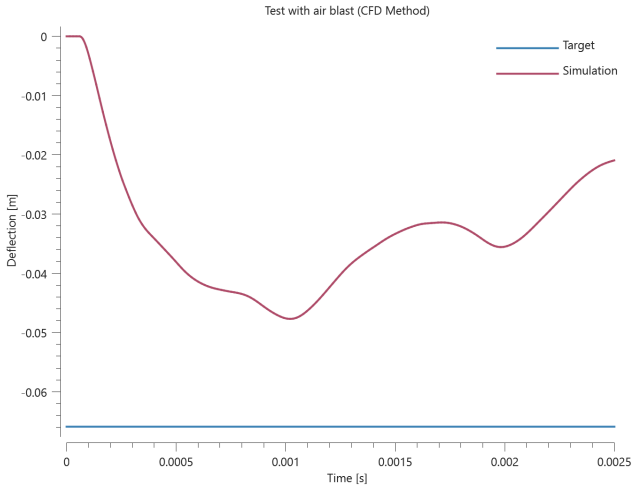

Figure 6. Deflection vs. time from simulation together with max deflection from experiment.

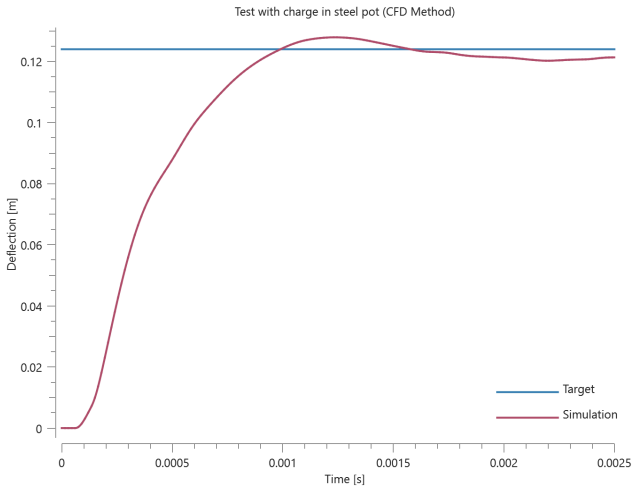

Figure 7. Deflection vs. time from simulation together with max deflection from experiment.

A convergence study regarding the number of CFD cells used is presented in Figure 8 and 9. Quarter symmetry is used. For version control, 0.40 cm sized cells are used.

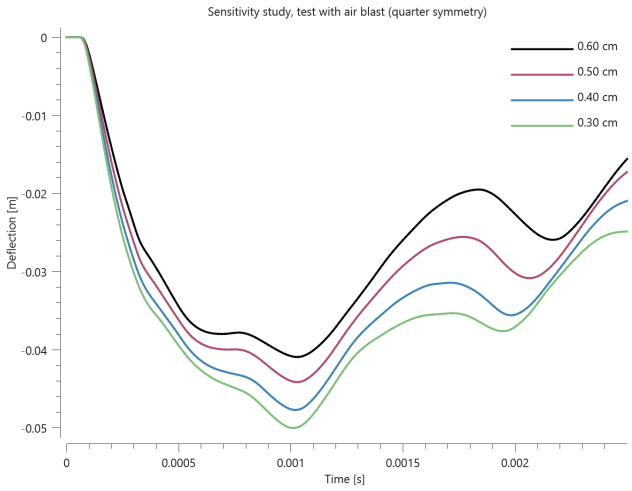

Figure 8. Deflection vs. time from simulations with 0.60 cm, 0.50 cm, 0.40 cm and 0.30 cm sized CFD cells.

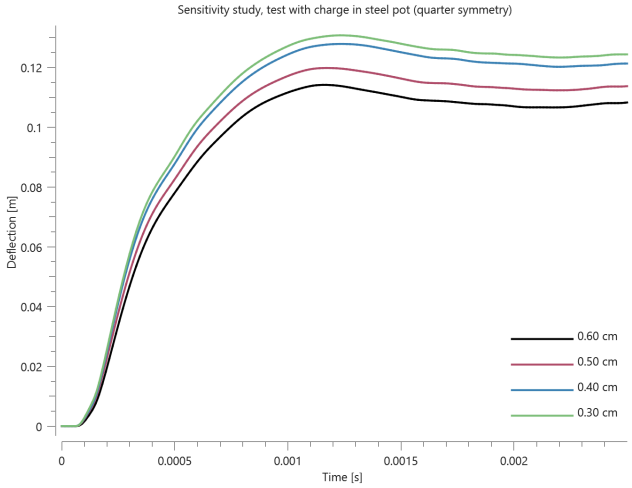

Figure 9. Deflection vs. time from simulations with 0.60 cm, 0.50 cm, 0.40 cm and 0.30 cm sized CFD cells.

References

[1] - Björn Zakrisson, Bengt Wikman, Hans-Åke Häggblad, Numerical simulations of blast loads and structural deformation from near-field explosions, International Journal of Impact Engineering, Volume 38, 2011, Pages 597-612.

TESTS

This benchmark is associated with 20 tests.

B. Zakrisson et al. (2012)

Modelling and simulation of explosions in soil interacting with deformable structures

In this investigation the results from Zakrisson et al (2012) are compared with numerical results from simulations. The setup is a charge buried in a box filled with sand. A steel plate is located above the

surface, and the peak displacement of the plate is measured. Stand-off distance (SoD) and depth of burial (DoB) is varied. The size of the box is adjusted to fit the charge at the different depths. The charge is a 750g cylinder of m/46, with a diameter-to-height ratio of 3. Experiment conditions are presented in Table 1 and an image of the model is displayed in Figure 1.

Run	Test	Sand Density ρ (kg/m^3)	Sand Moisture $mass$-%	Box Depth (m)	Box Width (m)	SoD (m)
1	1-2	1840 ± 17	7.9 - 8.2	0.5	0.95	0.246
2	3-5	1862 ± 40	6.9 - 8.3	0.5	0.95	0.246
3	6-8	1842 ± 17	7.3 - 7.5	0.6	0.95	0.235
4	9-10	1771 ± 5	0	0.5	0.95	0.235

Table 1. Experiment conditions.

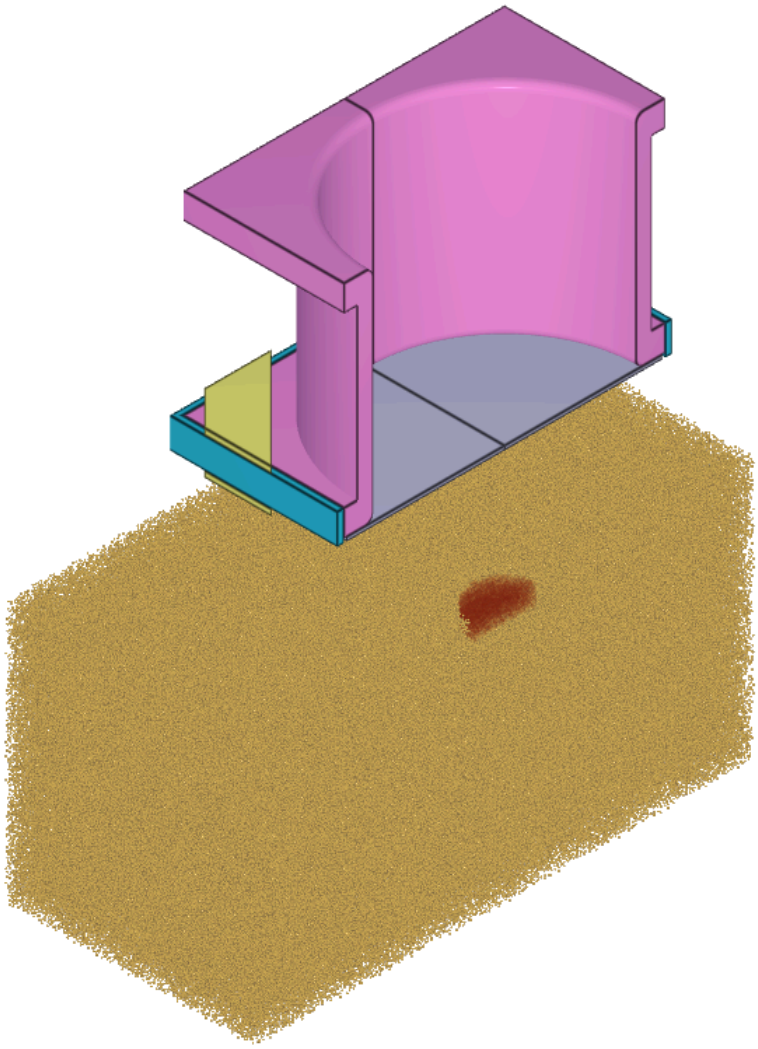

Figure 1. Half symmetry model of the test.

The target plate of steel is modeled in accordance to the referenced literature while the rig is modeled as rigid. The explosive charge and sand are modeled with 1M particles and quarter symmetry is used. Air is not included in any of the tests.

A user-defined sand is employed for Run 1-3. The sand is calibrated based on Run 1 and then used in Run 2 and 3. For run 4, the preset "dry" is used. The density of the sand in each model is adjusted to match the density of the sand used in the corresponding experiment. The sand domain in the model is open at the sides but closed at the bottom.

The max displacement found from the numerical models are compared to the experimental results in Table 2 and Figure 2 - 5.

Run	Test	Sand Type	Sand Density ρ (kg/m^3)	Max deflection Experiment (m)	Max deflection Simulation (m)	Error (%)
1	1-2	user	1840	0.092	0.087	-5.4
2	3-5	user	1862	0.103	0.097	-5.8
3	6-8	user	1842	0.072	0.075	4.2
4	9-10	dry	1771	0.092	0.089	-3.3

Table 2. Max deflection found in the experiments and the simulations.

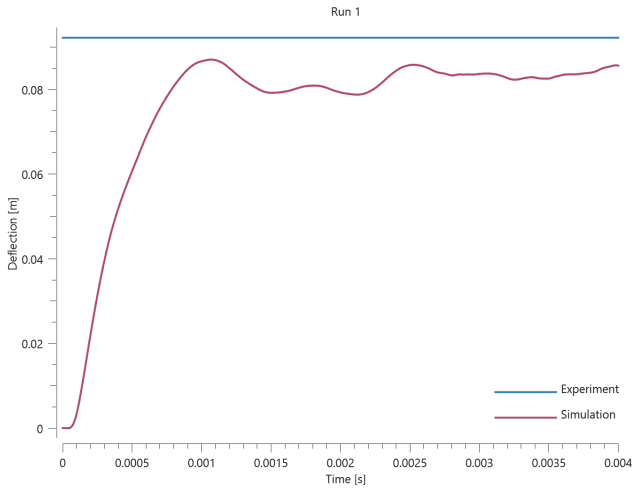

Figure 2. Deflection vs. time from simulation together with max deflection from experiment.

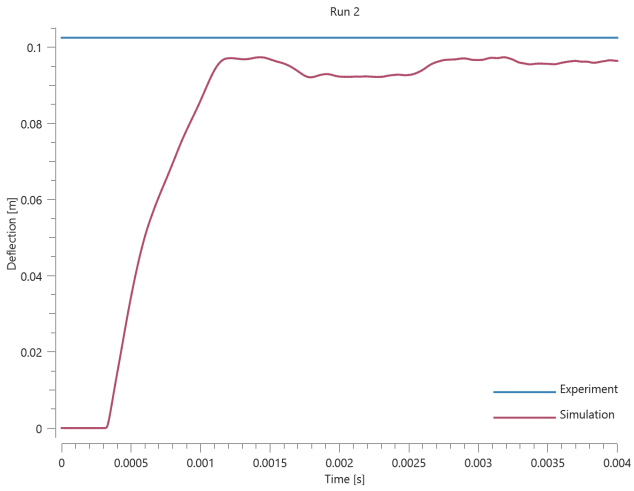

Figure 3. Deflection vs. time from simulation together with max deflection from experiment.

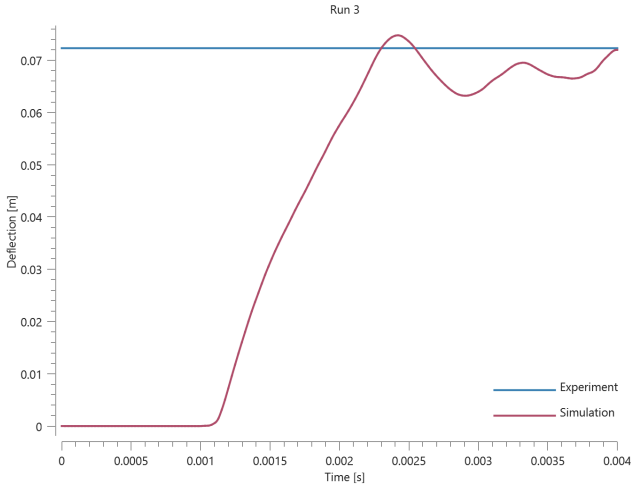

Figure 4. Deflection vs. time from simulation together with max deflection from experiment.

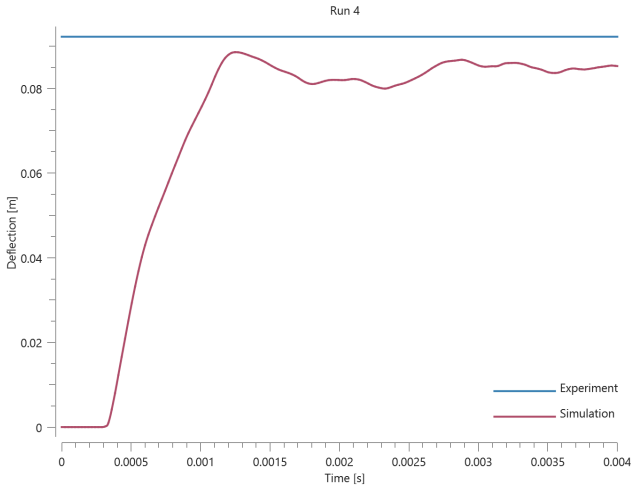

Figure 5. Deflection vs. time from simulation together with max deflection from experiment.

A sensitivity study regarding the number of particles used is done for Run 1 with results presented in Figure 6. For version control, 1M particles are used.

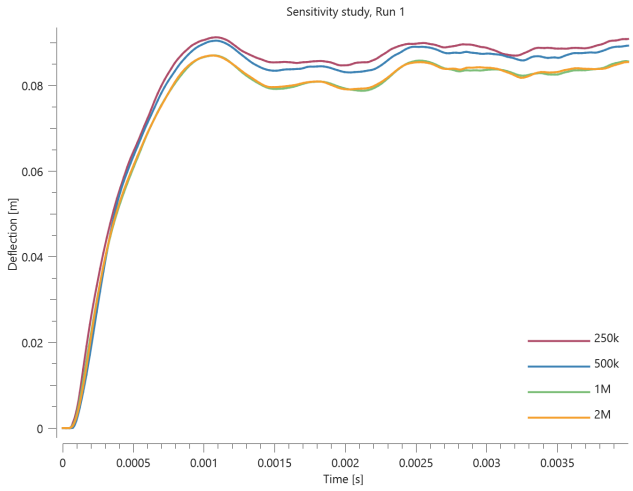

Figure 6. Deflection vs. time from simulations with 250k, 500k, 1M and 2M particles.

References

[1] - Björn Zakrisson, Hans-Åke Häggblad, Pär Jonsén, Modelling and simulation of explosions in soil interacting with deformable structures, Central European Journal of Engineering, Volume 2, 2012, Pages 532-550.

TESTS

This benchmark is associated with 8 tests.

C. E. Anderson et al. (2011)

Mine Blast Loading Experiments

In this investigation the results from Anderson et al (2011) are compared with numerical results from simulations. The setup is a charge buried in sand. Sand is filled in a cylindrical cardboard container and a thick target plate of steel is located a certain distance above the sand surface. The impulse from the blast on the plate is measured. Stand-off distance (SoD) is varied, and both flat and V-shaped plates are used, as shown in Figure 1. The charge is a cylinder of 625 g comp. B, with a diameter-to-height ratio of 3, and its top 20 cm below the sand surface. Four different cases are investigated, with conditions as described in Table 1.

Test	Sand Density	Sand Moisture -%	Plate Shape	Plate Mass	Plate SoD
1-3	1370 ± 30	7	Flat	300	0.30
4-6	1370 ± 30	7	Flat	300	0.30

Test	Sand Density ρ_s	Sand Moisture w_s -%	Plate Shape	Plate Mass m_p	Plate SoD μ_s
7-9	1370 ± 30	7	V-90°	308.4	0.25
10-12	1370 ± 30	7	V-120°	309.4	0.25

Table 1. Experiment conditions.

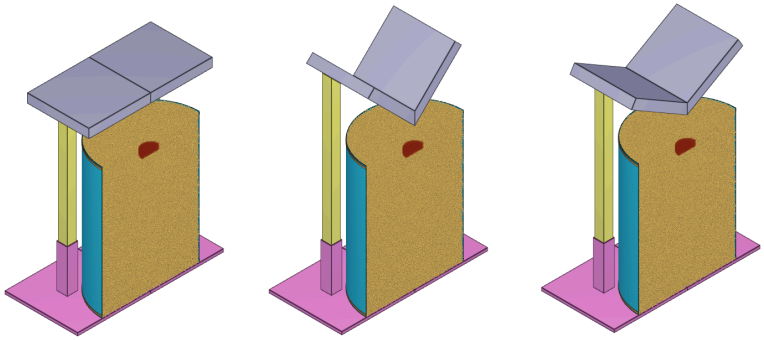

Figure 1. Half symmetry models. Three different configurations are investigated: flat plate (test 1-6), V-90 plate (test 7-9) and v-120 (test 10-12).

The target plate is modeled as rigid with a density of ~ $7800\ kg/m^3$. The cardboard is simplified as ideal plastic with a yield limit of 3 MPa and a failure strain of 5%. All cases are modeled with quarter symmetry, 2M particles and without air. Set against other experiments with dry sand (Neuberger (2007), Wadley (2011), Zakrisson (2011) and Rigby (2016)), the sand density in this investigation is unusually low. The preset "dry" is selected with a reduced density to match the density of the sand used in the experiments.

The impulse transfer to the target plate found in the numerical simulations are compared to the experimental results in Table 2 and Figure 2.

Test	Run	Experiment (Ns)	Simulation (Ns)	Error (%)
1-3	1	1979	1864.0	-5.8
4-6	2	1636	1636	-0.0
7-9	3	812	748.9	-7.8
10-12	4	1182	1171.1	-0.9

Table 2. Impulse vs. time from simulations with dry sand from latest version control.

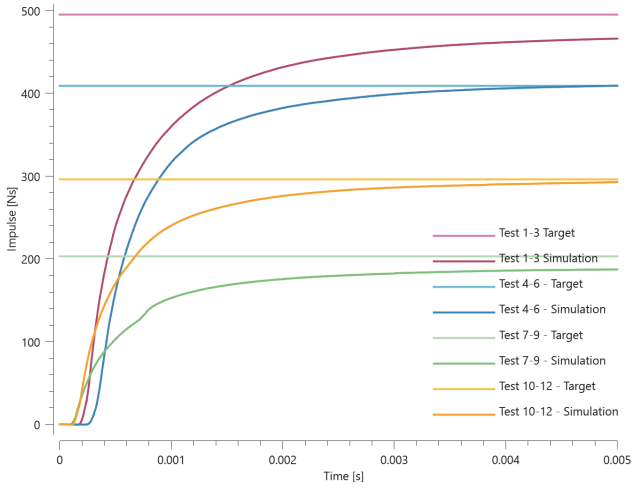

Figure 2. Impulse vs. time from simulations with dry sand from latest version control.

A sensitivity study regarding the number of particles has been done for Run 1 with results showed in Figure 3. For version control, 2M particles are used.

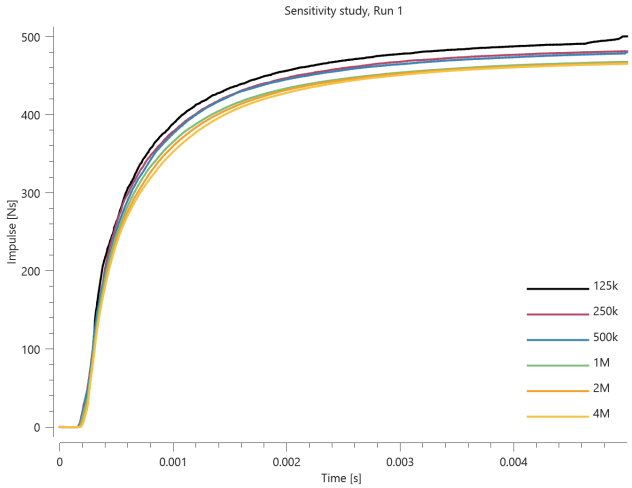

Figure 3. Impulse transfer vs. time for Run 1 with 125k, 250k, 500k, 1M, 2M and 4M particles.

References

[1] - C. E. Anderson Jr., T. Behner, C. E. Weiss, S. Chocron, R. P. Bigger, Mine Blast Loading: Experiments and Simulations, International Journal of Impact Engineering, Volume 38, 2011, Pages 697-706.

TESTS

This benchmark is associated with 10 tests.

H. N. G. Wadley et al. (2011)

A Discrete Particle Approach to simulate the Combined Effect of Blast and Sand Impact Loading of Steel Plates

In this investigation the results from Wadley et al (2011) are compared with numerical results from simulations. The setup is a spherical charge of 150 g C4 at various stand-off distances (15, 20 or 25 cm) from a stainless steel AL-6XN target plate, see Figure 1. The stand-off distance (SoD) is measured from center of charge to plate face.

The tests were divided into three groups. In the first group the high explosive (HE) was set off in air. In the second group the HE charge was surrounded by a spherical shape of dry sand. In the third group, the HE charge was surrounded by wet sand.

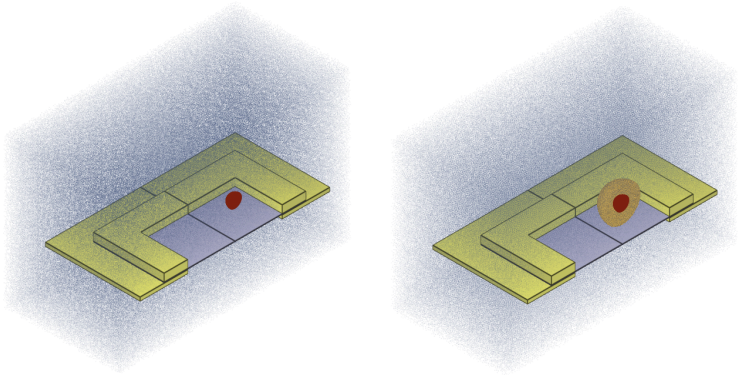

Figure 1. To the left: Model of air blast tests. To the right: Model of tests with sand surrounding the explosive charge.

The target plate is modeled with material data from the referenced article while the frame is modeled as rigid. All cases are modeled with quarter symmetry, 1M discrete particles and with air included. The sand presets "dry" and "wet" are used without any change in density since they match the densities of the sand types used in the experiments.

After the experiments the permanent deflection of the center part of the plate was measured. A comparison between the experimental and numerical results is presented in Table 1.

Test	Sand	Stand-off [illegible]	Deflection Experiment [illegible]	Deflection Simulation [illegible]	Error (%)
1	0	15	0.017	0.018	5.9
2	0	20	0.013	0.015	15.4
3	0	25	0.011	0.012	9.1
4	dry	15	0.039	0.034	-12.8
5	dry	20	0.027	0.026	-3.7

Test	Sand	Stand-off [m]	Deflection Experiment [m]	Deflection Simulation [m]	Error (%)
6	dry	25	0.019	0.019	0.0
7	wet	15	0.056	0.052	-7.1
8	wet	20	0.042	0.044	4.8
9	wet	25	0.035	0.035	0.0

Table 1. Permanent deflections found from the experiments and the simulations. (Discrete Particle Method).

The models sensitivity to the number of particles is investigated for the cases with the greatest stand-off distance (Test 3, 6 and 9). Results are presented in Figure 2, 3 and 4. For version control, 1M particles are used.

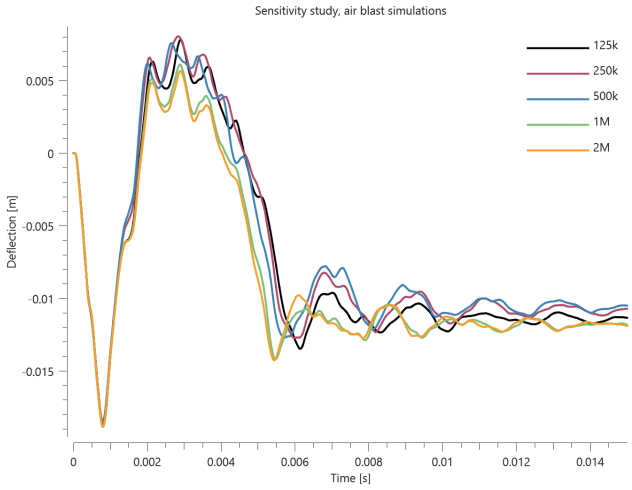

Figure 2. Deflection vs. time from air blast simulations with 125k, 250k, 500k 1M and 2M particles.

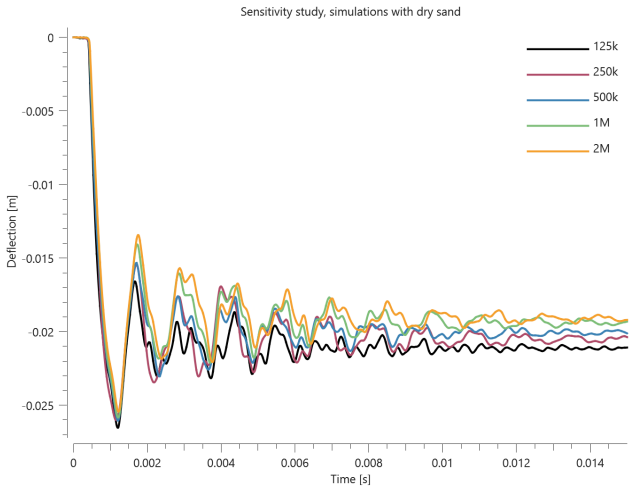

Figure 3. Deflection vs. time from simulations with dry sand with 125k, 250k, 500k 1M and 2M particles.

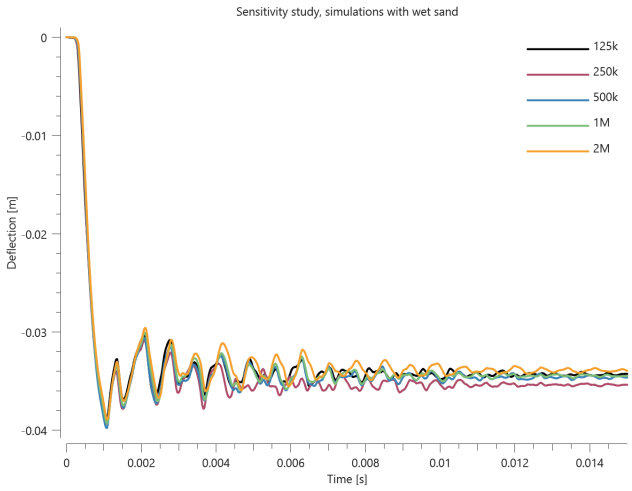

Figure 4. Deflection vs. time from simulations with wet sand with 125k, 250k, 500k 1M and 2M particles.

The permanent deflection of the center part of the plate from the CFD Method compared to the experimental results is presented in Table 2.

Test	Sand	Stand-off (cm)	Deflection Experiment (m)	Deflection Simulation (m)	Error (%)
1	0	15	0.017	0.021	23.5
2	0	20	0.013	0.018	38.5
3	0	25	0.011	0.013	18.2

Table 2. Permanent deflections found from the experiments and the simulations. (CFD Method).

The models sensitivity to the number of CFD cells is investigated for case 3. Results are presented in Figure 5. For version control, 0.50 cm sized cells are used.

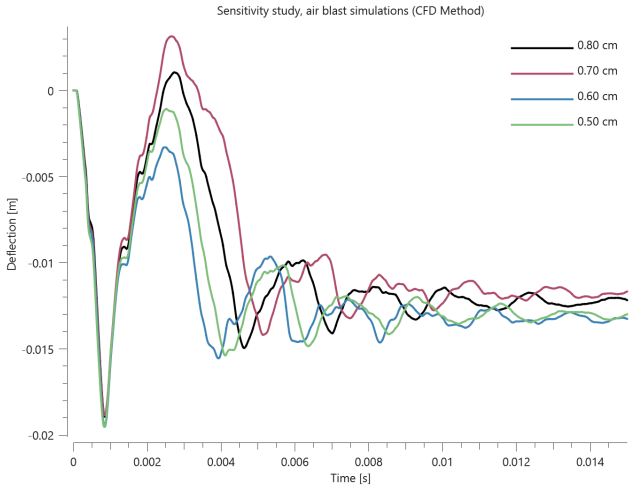

Figure 5. Deflection vs. time from air blast simulations with 0.80 cm, 0.70 cm, 0.60 cm and 0.50 cm sized CFD cells.

References

[1] - T. Børvik, L. Olovsson, A.G. Hanssen, K.P. Dharmasena, H. Hansson, H.N.G. Wadley, A discrete particle approach to simulate the combined effect of blast and sand impact loading of steel plates, Journal of the Mechanics and Physics of Solids, Volume 59, Issue 5, May 2011, Pages 940-958.

TESTS

This benchmark is associated with 31 tests.

K. Spranghers et al. (2013)

Numerical Simulation and Experimental Validation of the Dynamic Response of Aluminium Plates Under Free Air Explosions

In this investigation the results from Spranghers et al (2013) are compared with numerical results from simulations. The experiment includes a small spherical charge of 41 g C4 (including detonator) at a distance of 250 mm from an aluminium plate fixed in a frame, see Figure 1.

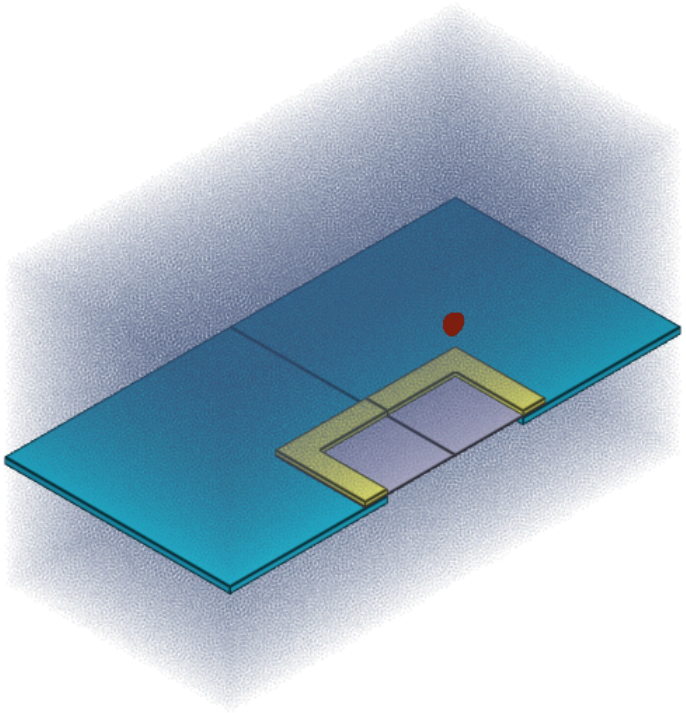

Figure 1. The numerical model of the experiment with the explosive charge, air, target plate and frame.

The aluminium target plate is modeled with material parameters from the referenced article and the frame is modeled as elastic with steel properties. The air and explosive charge are modeled with a total

of 500 k discrete particles. Quarter symmetry is utilized to reduce the computational time.

The maximum initial peak deflections, measured at center of plate, are compared in Table 1 and Figure 2. The experimental average is based on three out of four tests. The fourth is excluded as it provided a more flexible response compared to the others.

Test	Exp. average of 3 tests (m)	Simulation (m)	Error (%)
Airblast	0.021	0.017	-19.0

Table 1. Maximum initial peak deflection (Discrete Particle Method).

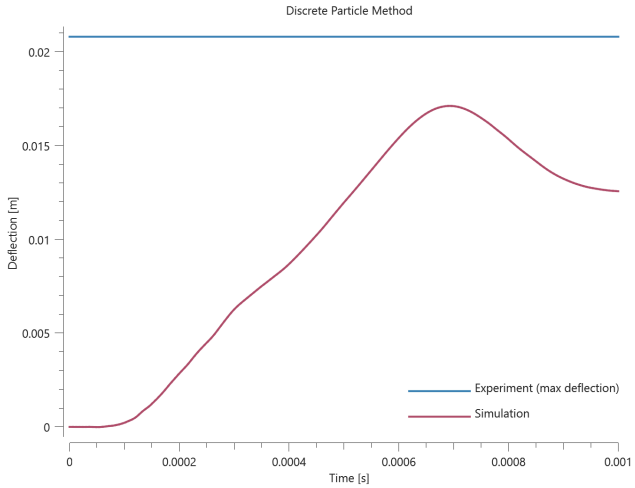

Figure 2. Deflection vs. time from simulation together with max deflection from experiment.

The numerical models sensitivity to the number of particles used has been investigated with results presented in Figure 3. For version control 500k particles are used.

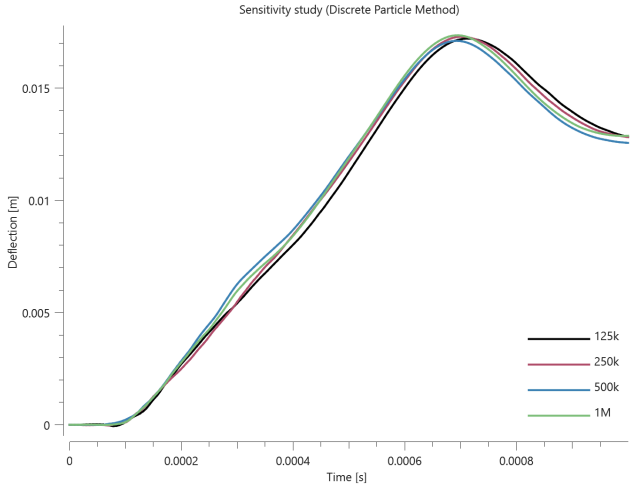

Figure 3. Deflection vs. time from simulations with 125, 250, 500k and 1M particles.

The maximum initial peak deflections at center of the plate from the CFD method is presented in Table 2 and Figure 4.

Test	Exp. average of 3 tests (m)	Simulation (m)	Error (%)
Airblast	0.021	0.018	-14.3

Table 2. Maximum initial peak deflection (CFD Method).

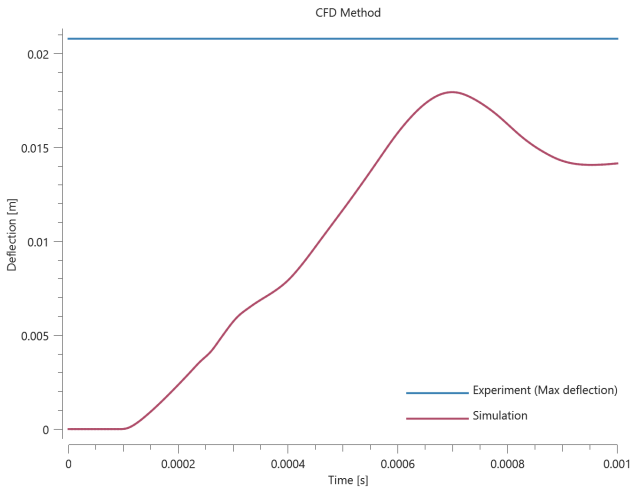

Figure 4. Deflection vs. time from simulation together with max deflection from experiment.

The numerical models sensitivity to the number CFD cells used is investigated with results presented in Figure 5. For version control, 0.30 cm sized cells are used.

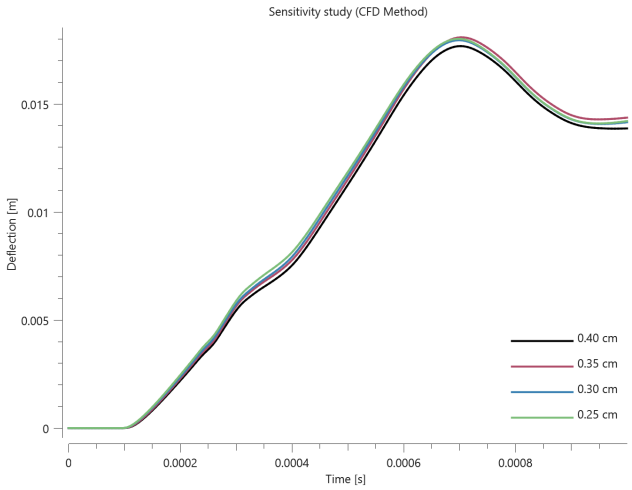

Figure 5. Deflection vs. time from simulations with 0.40 cm, 0.35 cm, 0.30 cm and 0.25 cm sized CFD cells.

References

[1] - K. Spranghers, I. Vasilakos, D. Lecompte, H. Sol, J. Vantomme, Numerical simulation and experimental validation of the dynamic response of aluminium plates under free air explosions, International Journal of Impact Engineering, Volume 54, April 2013, Pages 83-95.

TESTS

This benchmark is associated with 10 tests.

M. Held (2002)

```
##### Near Field Explosions
```

In this investigation the results from G.W. Weaver and W. P. Walters (1987) and M. Held (2002) are compared with numerical results from simulations. The experiments consist of an cylindrical explosive charge with length L_e and diameter D_e. A steel disc with thickness T_d and diameter D_d is located at a distance d from the explosive charge with its axial direction aligned with the cylindrical charge. The test setup is presented in Figure 1.

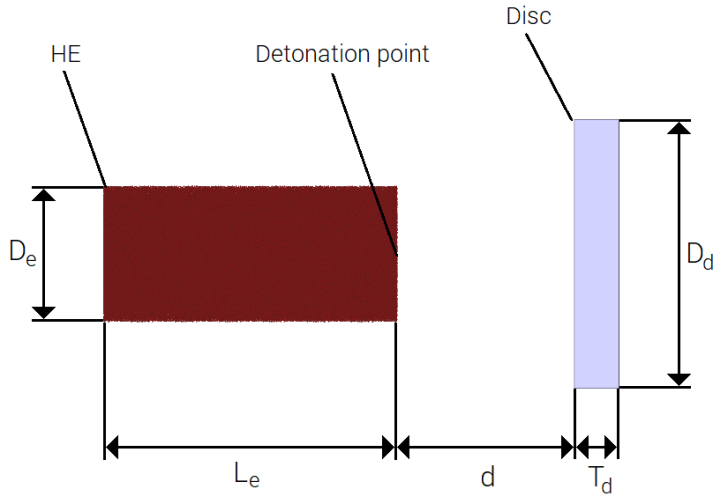

Figure 1. The test setup.

The thickness of the disc, charge mass and the distance between the charge and the disc are altered in a total of 15 configurations, as presented in Table 1. A disc diameter of 152.4 mm and an Octol 78/22 charge with a length-to-diameter ratio of 2.16 is used in all cases.

Test	Disc thickness, (T_d) (mm)	Mass of explosive (kg)	Charge diameter, (D_c) (mm)	Distance, (d) (m)	Scaled distance $m/kg^{1/3}$
1	25.4	1.39	76.2	0.1	0.089
2	19.1	1.39	76.2	0.1	0.089
3	12.7	1.39	76.2	0.1	0.089
4	6.4	1.39	76.2	0.1	0.089
5	25.4	1.39	76.2	0.05	0.044
6	12.7	1.39	76.2	0.05	0.044
7	25.4	1.39	76.2	0.075	0.067
8	12.7	1.39	76.2	0.075	0.067
9	25.4	0.79	63.5	0.1	0.108
10	25.4	0.79	63.5	0.075	0.081
11	25.4	0.79	63.5	0.05	0.054
12	25.4	1.72	82.6	0.1	0.083
13	25.4	1.72	82.6	0.05	0.041
14	12.7	1.72	82.6	0.1	0.083
15	12.7	1.72	82.6	0.05	0.041

Table 1. Four different discs, three different explosive charges and three distances are investigated.

The disc is modeled as a high strength steel and the explosive is modeled with 500k discrete particles. Air is not included in any test. Figure 2 shows the initial state of the simulation with the particle domain boundaries visualized with black lines.

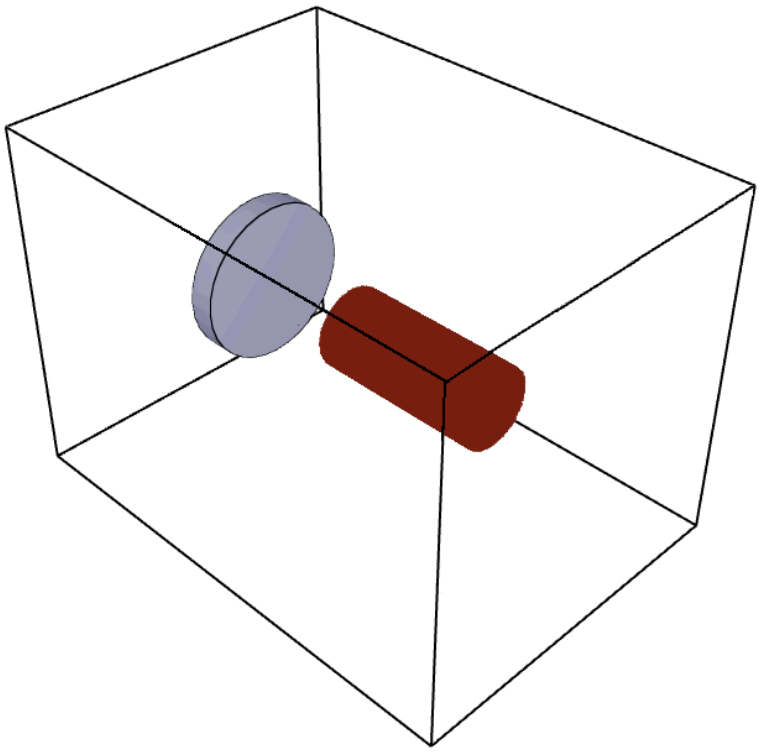

Figure 2. Inital state of the simulation.

The maximum velocity and impulse found from the simulations are compared to experimental data in Table 2 and in Figure 3 and 4.

Test	Experiment velocity	Experiment Impulse	Simulation Velocity	Simulation Impulse	Error velocity (%)	Error Impulse (%)
1	58	210	63.1	226.6	8.8	7.9
2	72	198	83.7	226.1	16.3	14.2
3	114	207	123.8	222.2	8.6	7.3
4	207	187	237.5	214.9	14.7	14.9
5	83	299	86.3	309.8	4.0	3.6
6	171	310	170.9	306.9	-0.0	-1.0
7	73	266	73.2	263.0	0.3	-1.1
8	133	241	144.3	259.0	8.5	7.5

Test	Experiment velocity [m/s]	Experiment Impulse [Ns]	Simulation Velocity [m/s]	Simulation Impulse [Ns]	Error velocity (%)	Error Impulse (%)
9	33	120	39.4	141.4	19.4	17.9
10	40	143	46.1	165.4	15.2	15.7
11	47	172	53.4	191.8	13.6	11.5
12	63	228	75.0	269.2	19.0	18.1
13	100	368	102.3	367.3	2.3	-0.2
14	112	204	147.3	264.5	31.5	29.6
15	201	365	201.4	361.6	0.2	-0.9

Table 2. Maximum impulse and velocity found in the experiments and the simulations (Discrete Particle Method).

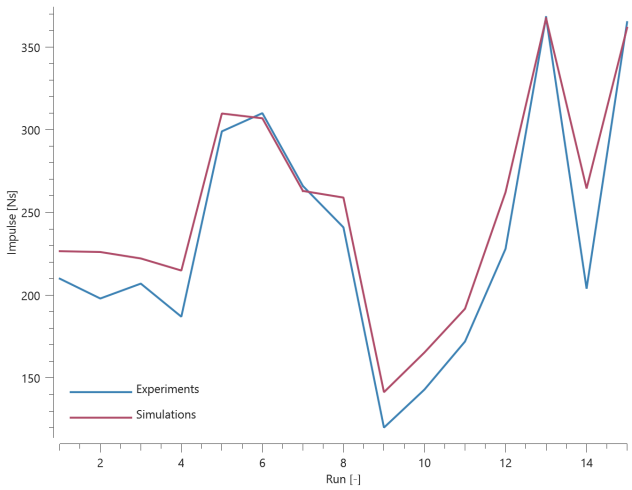

Figure 3. Comparison of impulse between simulations and experiments.

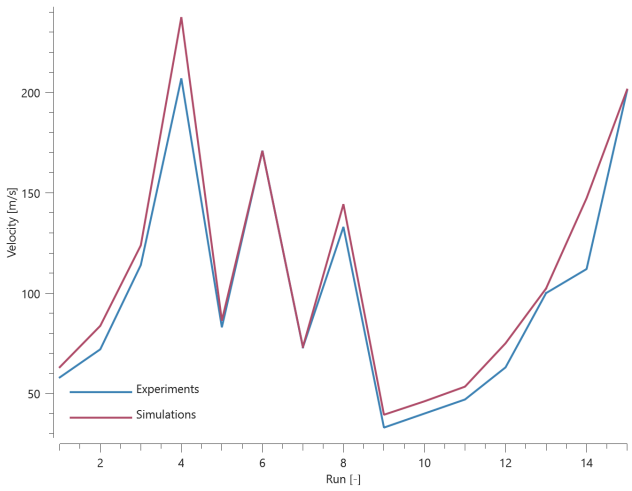

Figure 4. Comparison of velocity between simulations and experiments.

Convergence was investigated for Test 9 with results presented in Figure 5. For version control, 500k particles are used.

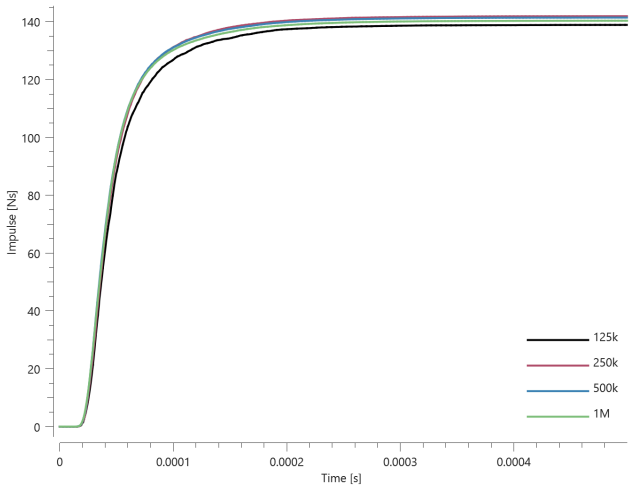

Figure 5. Impulse vs. time for simulations of Test 9 with 125k, 250k, 500k and 1M particles.

The maximum velocity and impulse from the CFD method is compared to experimental data in Table 3 and in Figure 6 and 7.

Test	Experiment velocity	Experiment Impulse	Simulation Velocity	Simulation Impulse	Error velocity (%)	Error Impulse (%)
1	58	210	57.8	207.6	-0.3	-1.2
2	72	198	77.5	209.2	7.6	5.7
3	114	207	117.8	211.5	3.4	2.2

Test	Experiment velocity	Experiment Impulse	Simulation Velocity	Simulation Impulse	Error velocity (%)	Error Impulse (%)
4	207	187	235.2	212.8	13.6	13.8
5	83	299	80.3	288.3	-3.3	-3.6
6	171	310	160.6	288.4	-6.1	-7.0
7	73	266	69.1	248.1	-5.3	-6.7
8	133	241	133.8	240.2	0.6	-0.3
9	33	120	33.6	120.7	1.9	0.6
10	40	143	40.7	146.0	1.7	2.1
11	47	172	48.4	173.8	3.0	1.0
12	63	228	70.4	252.8	11.7	10.9
13	100	368	99.3	356.5	-0.7	-3.1
14	112	204	144.4	259.2	28.9	27.1
15	201	365	20.7	360.3	-0.1	-1.3

Table 3. Maximum impulse and velocity found in the experiments and the simulations (CFD Method).

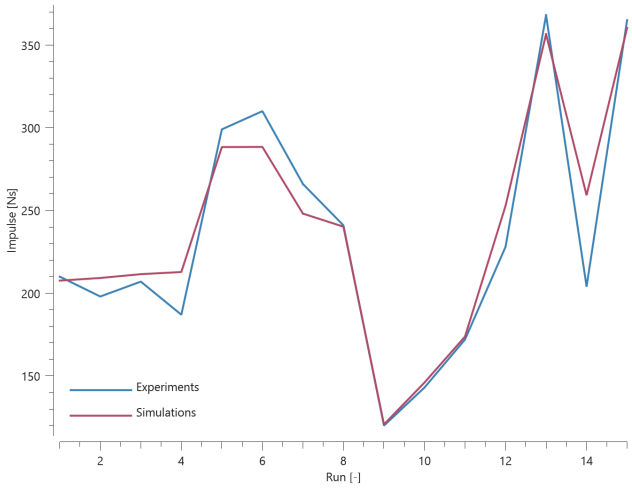

Figure 6. Comparison of impulse between simulations and experiments.

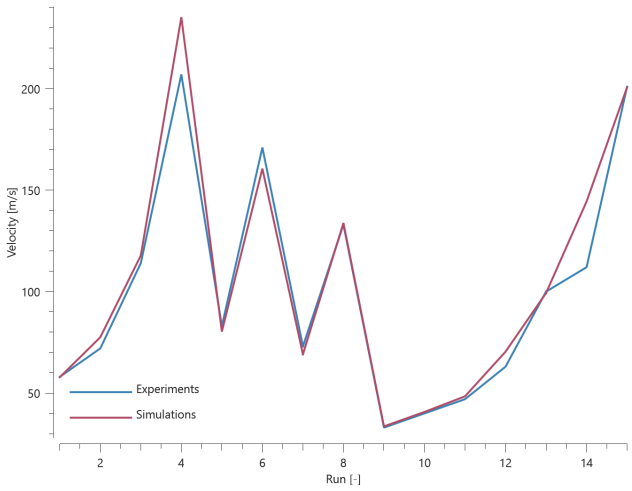

Figure 7. Comparison of velocity between simulations and experiments.

Convergence was investigated for Test 1 with results presented in Figure 8. For version control, 0.15 cm sized cells are used.

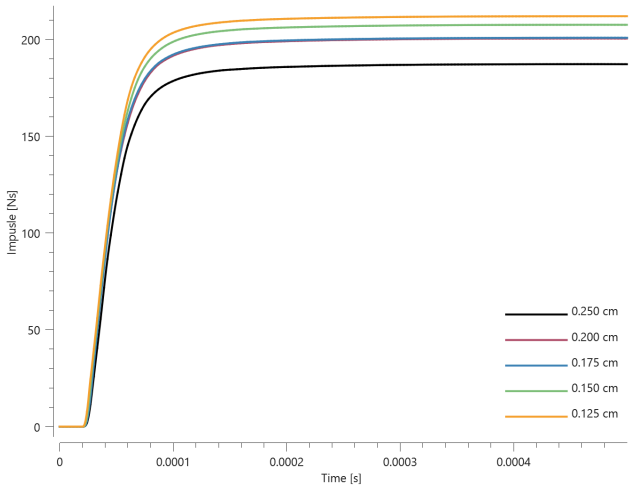

Figure 8. Impulse vs. time for simulations of Test 1 with 0.250 cm, 0.200 cm, 0.175 cm, 0.150 cm and 0.125 cm sized CFD cells.

References

[1] - M. Held, Near Field Explosions, Propellants, Explosives, Pyrotechnics 27, 2002, page 244-246.

[2] - G.W. Weaver and W. P. Walters, Proximate Blast Loading of Structures, 10th International Symposium on Ballistics, San Diego, CA, 1987, page 27-29.

TESTS

This benchmark is associated with 39 tests.

S. E. Rigby et al. (2016)

Measuring Spatial Pressure Distribution from Explosives Buried in Dry Leighton Buzzard Sand

In this investigation the results from Rigby et al (2016) are compared with numerical results from simulations. The experiments include a 78 g PE4 charge with a diameter-to-height ratio of 3, buried in sand at a depth of 28 mm, measured from top of charge to sand surface. The sand is in a cylindrical steel container with an inner diameter of 500 mm, wall thickness of 30 mm and a height of 375 mm. Pressure and specific impulse is measured at the surface of a circular steel target plate with a diameter of 1.4 m and a thickness of 0.1 m.

In the experiment, data were extracted by 17 Hopkinson pressure bars that were installed in the plate. The holes in which the bars are inserted forms a cross with four sets of four holes in perpendicular arrays around a center hole. An illustration of the experimental setup is presented in Figure 1.

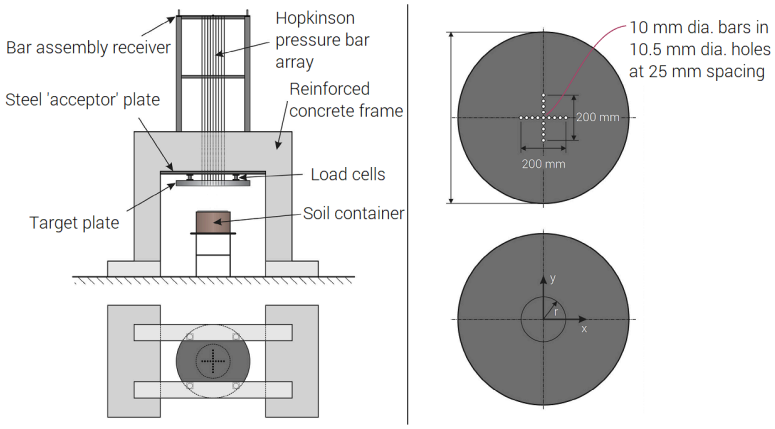

Figure 1. Illustration of the experimental set-up.

Two stand-off distances (SoD) are investigated, and five tests are executed at each distance. The test configurations are summarized in Table 1.

Test	Sand Density ρ (kg/m^3)	Sand Moisture $mass$-%	Explosive Type	Explosive Mass (kg)	Explosive Shape	SoD (m)	DoB (m)
1-5	1640	2.5	PE4	0.078	3:1 cylinder	0.168	0.028
6-10	1640	2.5	PE4	0.078	3:1 cylinder	0.133	0.028

Table 1. Conditions in the experiments.

The sand preset "dry" is used with an adjusted density to match the density of the sand in the experiments. The sand and explosive are modeled with 4M particles and the models are run without air included.

The pressure and specific impulse is extracted from the simulations by nine sensors (*OUTPUT_SENSOR). Four sensors are positioned in two perpendicular arrays from a sensor at the center of the plate. The pressure and the specific impulse is averaged from the two sensors located at the same radial distance.

Numerical and experimental results of the specific impulse vs. radial position is presented in Figure 2 for Test 1-5 and Figure 3 for Test 6-10.

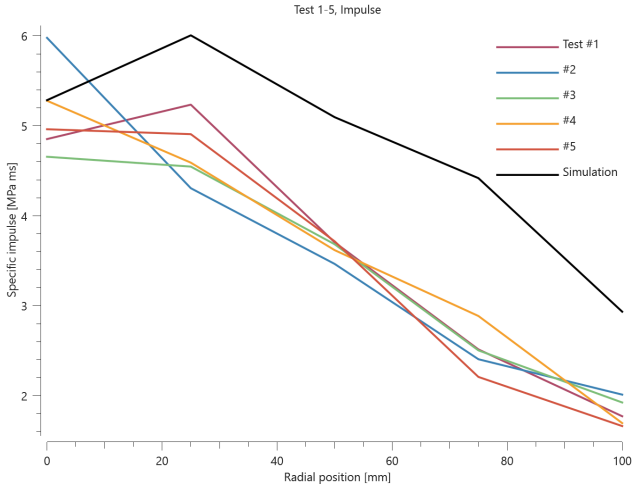

Figure 2. Impulse intensity vs. radial position from test 1-5.

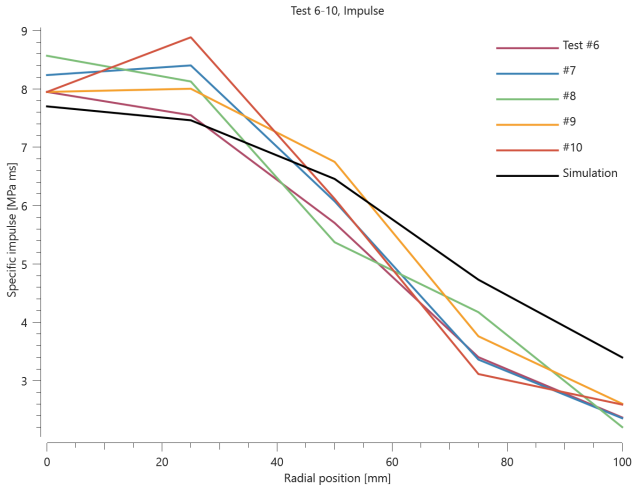

Figure 3. Impulse intensity vs. radial position from test 6-10.

References

[1] - S.E. Rigby, S.D. Fay, S.D. Clarke, A. Tyas, J.J. Reay, J.A. Warren, M. Gant, I, Elgy, Measuring spatial pressure distribution from explosives buried in dry Leighton Buzzard sand, International Journal of Impact Engineering, Volume 96, 2016, Pages 89-104.

TESTS

This benchmark is associated with 2 tests.